ORIGINAL RESEARCH

CLINICAL ORAL IMPLANTS RESEARCH **WILEY**

Fully guided implant surgery using Magnetic Resonance Imaging – An in vitro study on accuracy in human mandibles

Tabea Flügge[1,2] 🔵 | Ute Ludwig[3] 🔵 | Gita Winter[1] | Philipp Amrein[3] | Florian Kernen[1] 🔵 | Katja Nelson[1]

[1]Department of Oral and Maxillofacial Surgery, Translational Implantology, Medical Center–University of Freiburg, Faculty of Medicine–University of Freiburg, Freiburg, Germany

[2]Department of Oral and Maxillofacial Surgery, Charité–Universitätsmedizin Berlin, Corporate Member of Freie Universität Berlin, Humboldt-Universität zu Berlin, Berlin Institute sof Health, Berlin, Germany

[3]Department of Radiology, Medical Physics, Medical Center–University of Freiburg, Faculty of Medicine–University of Freiburg, Freiburg, Germany

Correspondence
Tabea Flügge, Department of Oral and Maxillofacial Surgery, Translational Implantology, University Medical Center Freiburg, Hugstetter Straße 55, Freiburg 79106, Germany.
Email: tabea.fluegge@uniklinik-freiburg.de

Funding information
International Team for Implantology, Grant/Award Number: 1241_2017

Abstract

Objectives: The objective of this in vitro study was to assess the accuracy of fully guided implant placement following virtual implant planning based on MRI.

Material and Methods: Sixteen human cadaver hemimandibles with single missing teeth ($n = 3$), partially edentulous ($n = 6$) and edentulous situations ($n = 7$) were imaged using MRI. MRI and optical scans obtained with an intraoral scanner, were imported into an implant planning software. Virtual prosthetic and implant planning were performed regarding hard- and soft-tissue anatomy. Drill guides were manufactured, and fully guided implant placement was performed. Buccal and lingual bone and implant nerve distance were measured by three examiners in preoperative MRI and postoperative CBCT. The implant position was assessed using a software for deviation of implant positions displayed in CBCT and optical scans, respectively.

Results: MRI displayed relevant structures for implant planning such as cortical and cancellous bone, inferior alveolar nerve and neighboring teeth. Implant planning, CAD/CAM of drill guides and guided implant placement were performed. Deviations between planned and actual implant positions in postoperative CBCT and optical scans were 1.34 mm (*SD* 0.84 mm) and 1.03 mm (*SD* 0.46 mm) at implant shoulder; 1.41 mm (*SD* 0.88 mm) and 1.28 mm (*SD* 0.52 mm) at implant apex, and 4.84° (*SD* 3.18°) and 4.21° (*SD* 2.01°). Measurements in preoperative MRI and postoperative CBCT confirmed the compliance with minimum distances of implants to anatomical structures.

Conclusions: Relevant anatomical structures for imaging diagnostics in implant dentistry are displayed with MRI. The accuracy of MRI-based fully guided implant placement in vitro is comparable to the workflow using CBCT.

KEYWORDS
computer-aided design, guided implant surgery, magnetic resonance imaging, virtual implant planning

1 | INTRODUCTION

Magnetic resonance imaging (MRI) is a non-ionizing method to acquire three-dimensional images of human anatomy. Previous studies have shown high resolution and accurate display of the dento-alveolar complex (Flügge et al., 2016; Hövener et al., 2012; Ludwig et al., 2016). This study was conducted to confirm the feasibility of MRI-based virtual implant planning and assess the accuracy of fully guided implant placement in human mandibles ex vivo.

To date, virtual implant planning relies on radiologic data, namely computed tomography (CT) or cone beam computed tomography (CBCT), for the assessment of the bone. Radiologic techniques display mineralized tissues of the dento-alveolar complex including teeth, cancellous and cortical bone and the mandibular canal bearing the inferior alveolar nerve. For dental implant planning, (CB-)CT is complemented with optical scans of the teeth and the mucosal surface. The optical scan is essential as it adds information on soft tissue surfaces, the surface of the teeth and it is used for the design of drill guides for fully guided implant placement. Prior to actual implant planning, (CB-)CT data and optical scans are aligned using common surface characteristics.

Limitations in the workflow of virtual implant planning and fully guided implant placement are the occurrence of artifacts in (CB-)CT data and the missing information on soft tissues especially in (CB-)CT data, whereas Multislice-CT may display soft tissues. Artifacts occur in relation to dental restorations distorting not only the affected tooth, but the complete image volume (Nkenke et al., 2004; Schulze et al., 2011).

Novel and specified MR imaging protocols have been developed to promote MRI as an alternative imaging modality in dentistry (Flügge et al., 2016; Hövener et al., 2012; Ludwig et al., 2016). One major drawback of MRI is the poor visibility of structures with a low content of hydrogen, for example, teeth, which can only be displayed as signal voids using standard MR imaging techniques. Furthermore, image artifacts originate from metallic restorations and may hinder adequate interpretation of MR images and a lower image resolution is frequently found in MRI without specific intraoral coils compared to (CB)CT. The recent application of MRI in dentistry successfully showed the display of dental hard and soft tissues in high-resolution images by using dedicated coils (Bracher et al., 2011; Gruwel et al., 2007; Idiyatullin et al., 2011; Idiyatullin, Corum, Nixdorf, & Garwood, 2014; Tymofiyeva et al., 2008, 2009; Weiger et al., 2012). The use of MRI in clinical routine is, however, still limited due to extensive hardware requirements and high costs. Although, MR imaging is able to accurately display oral structures, the workflow for virtual implant planning and fully guided implant placement has not yet been described.

The first hypothesis of the present study was that dento-alveolar anatomy is sufficiently displayed using MRI to plan dental implants. The second hypothesis was that the workflow for fully guided implant surgery is feasible on the basis of MR imaging and optical surface scans. The third hypothesis was that the accuracy of fully guided implant surgery with MRI is within the range found in literature describing the accuracy of fully guided implant placement based on CBCT. Therefore, the aims of this study were (a) to test the feasibility of the workflow of virtual implant planning and fully guided implant surgery (b) to test the accuracy of fully guided implant placement based on MRI in vitro.

2 | MATERIALS AND METHODS

MR imaging, virtual implant planning and fully guided implant surgery was performed in 16 human hemimandibles. The specimens were supplied by the anatomical institute of the Albert-Ludwigs-University Freiburg. The study protocol was approved by the Institutional Review Board of Medical Center – University of Freiburg, Freiburg, Germany (338/13). The study was conducted in compliance with SRQR guidelines accessible through the EQUATOR network. Seven hemimandibles with an edentulous alveolar ridge (ED), 6 hemimandibles with a partially edentulous cantilever situation (PE) and three hemimandibles with a single missing tooth with neighboring teeth (ST) were included.

2.1 | Preparation of specimens

The specimens were conserved in 0.1% phenoxyethanol solution. Radio-opaque markers (MR/CT-PinPoint® Nr.128, Beekley Medical)
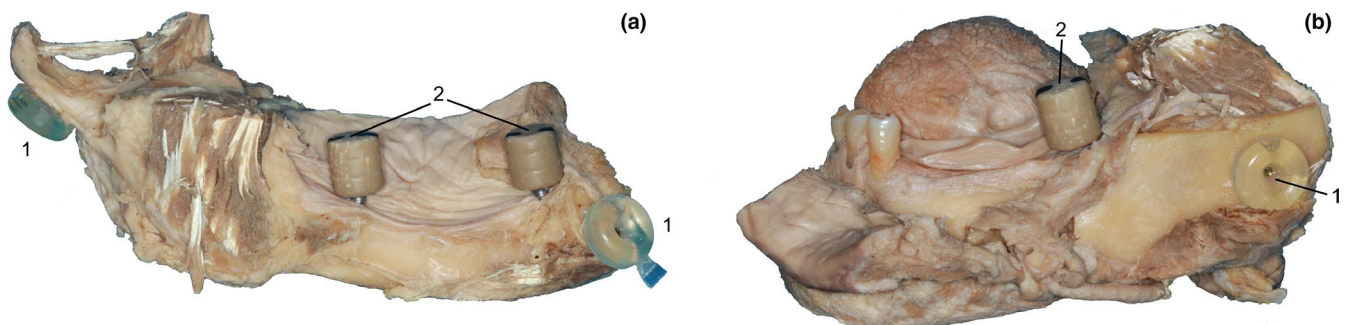
FIGURE 1 Anatomical specimens of human hemimandibles with edentulous alveolar ridge (a) with two resin posts (2) from lingual viewpoint and partially edentulous cantilever situation (b) with one resin post (2) from lateral viewpoint. Both specimens contain radio-opaque markers (1)

for image alignment that were visible in CBCT, MRI and optical scans were fixated to the hemimandibles outside of the region of interest using titanium osteosyntheses screws (25-875-11-75, KLS Martin).

Edentulous hemimandibles received two mini implants (Camlog) each for the support of drill guides. Hemimandibles with a cantilever situation received one distally positioned mini implant for drill guide support. Hemimandibles with one missing tooth and neighboring teeth did not receive mini implants. The mini implants were equipped with individually prefabricated adhesively fixated resin cylinders (length 10 mm, diameter 10 mm) (Technovit 4000, Heraeus Kulzer) (Figure 1).

2.2 | MR imaging and optical surface scans

Preoperative MR imaging was performed with individualized imaging protocols. Each hemimandible was scanned with a clinical whole-body MR system (Magnetom Prisma, Siemens Healthineers) equipped with a body transmit coil and a standard 20 channel head coil. 3D fast low flip angle shots (FLASH) sequences with the following imaging parameters were applied: echo time (TE) = 3.4 ms; repetition time (TR) = 8.7 ms; voxel size = $0.6 \times 0.6 \times 0.6$ mm^3; field of view 150 mm^2; flip angle = 15°; bandwidth = 280 Hz/px; acquisition time = 2:22 min. MRI data was available in DICOM-format.

Optical scans of the specimens were acquired with an intraoral scanner (Trios 3, 3Shape). The scanning sequence was started at the most distal aspect of the alveolar ridge and continued to the mesial aspect without interruption. The radiopaque markers were included in the optical scan. Scans were exported in the stl-data format.

2.3 | Virtual implant planning

The workflow of virtual implant planning, drill guide fabrication and fully guided implant insertion was performed as previously described (Flügge, Nelson, Schmelzeisen, & Metzger, 2013).

Virtual implant planning was performed with coDiagnostiX software (Version 7, Dentalwings). MR data and optical surface scans were imported with the software and aligned in a common coordinate system by selecting three corresponding regions visible in MR images and in optical scans. The keratinized mucosal surface and the radio-opaque markers were used for alignment. A fully digital prosthetic set-up for the missing teeth was performed and implants were positioned regarding the prosthetic set-up and the bone dimensions.

Diagnostic findings were discussed between the three examiners and a radiologist. The inferior alveolar nerve was defined in MR images and marked with the software tool for nerve canal detection (Figure 2). A distance of the implant apex to the inferior alveolar nerve of 2 mm was attempted, however, a shorter distance (min 1.4 mm) was accepted in cases of severe bone atrophy in partially and fully edentulous mandibles. Implants were placed to maintain a buccal and a lingual bone lamella and angulated to keep minimum distances to neighboring teeth if present. Implants were selected according to the dimension of the bone (Art-Nr. 021.4308; 021.4310, Bone Level Tapered, Straumann).

2.4 | Fabrication of drill guides

The original drill sleeves for fully guided implant surgery (Art-Nr. 034.053V4, Straumann) were selected. A distance of 4 mm between the implant shoulder and the drill sleeve was adjusted. The default protocol for drill guide design was conducted in the software. Areas of drill guide support were selected on the optical surface scans and an offset of 0.1 mm and a drill guide thickness of 3 mm was chosen. The resulting drill guide had a predetermined cut out for the drill sleeves and the tooth or mucosal surface, respectively that served for the control of the fit. The virtually designed drill guides were exported in an stl-format and produced using a biocompatible resin (MD610, Stratasys) with a polyjet 3D printer (Eden 260V, Stratasys) as previously described (Flügge et al., 2013).
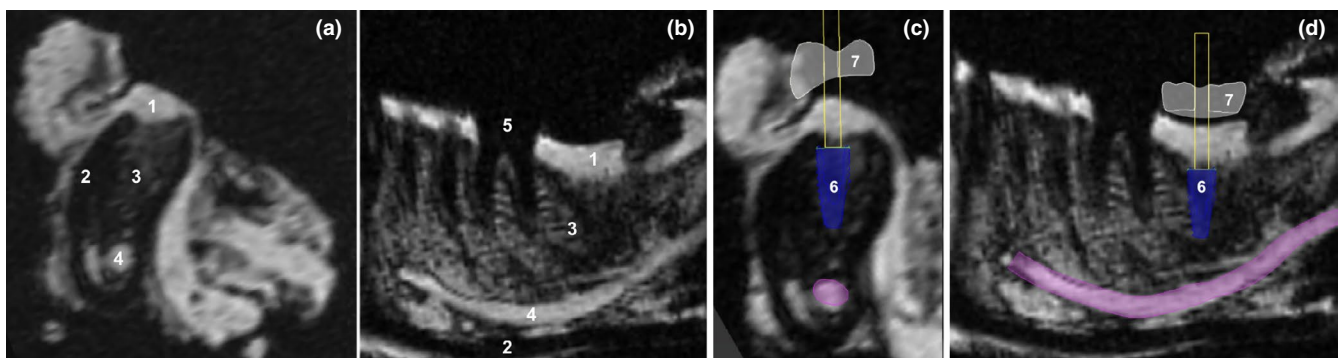
FIGURE 2 MR cross-sectional images in coronal (a,c) and sagittal (b, d) directions. The coronal cross-sections (a,c) show cortical bone (2) and cancellous bone (3), crestal gingiva (1) with surrounding mucosa. The distance between the planned implant (6) and the inferior alveolar nerve (4) and the buccal and lingual bone dimensions are assessed. The sagittal images show the long axis of the planned implant in region 37, the neighboring tooth (5) and the inferior alveolar nerve (4)
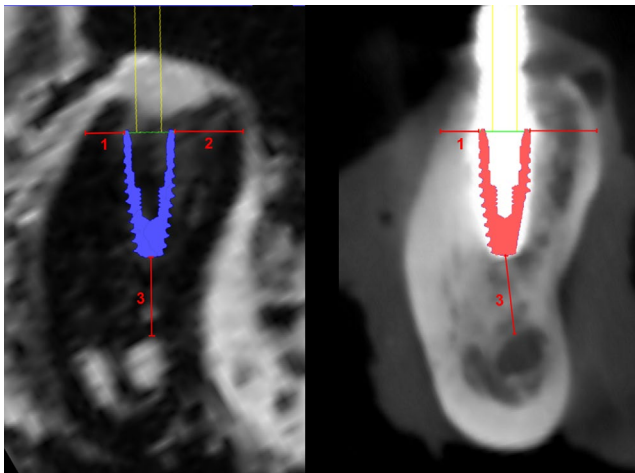
FIGURE 3 Measurement of buccal bone (1) and lingual bone (2), respectively, and implant apex to inferior alveolar nerve (3) in preoperative MR images (a) and postoperative CBCT images (b)

2.5 | Fully guided implant surgery

The fit of drill guides was visually verified on the specimens. A crestal mucoperiostal incision with mesial and distal releasing incisions was performed. A mucoperiostal flap was prepared and drill guides were inserted. Implant beds were incrementally prepared with the respective drilling protocol through the drill sleeve without removal and repositioning of drill guides. Implants were manually inserted through the drill sleeves using a torque-controlled ratchet (35 Ncm). The drill guides were removed after reaching the final implant position and removal of the insertion tool.

2.6 | Postoperative imaging and evaluation of implant positions

Postoperative CBCT imaging was performed (3D Accuitomo 170) with the following imaging protocol: image resolution 250 μm, 80 kV, 2 mA, FOV 140×100 mm^2.
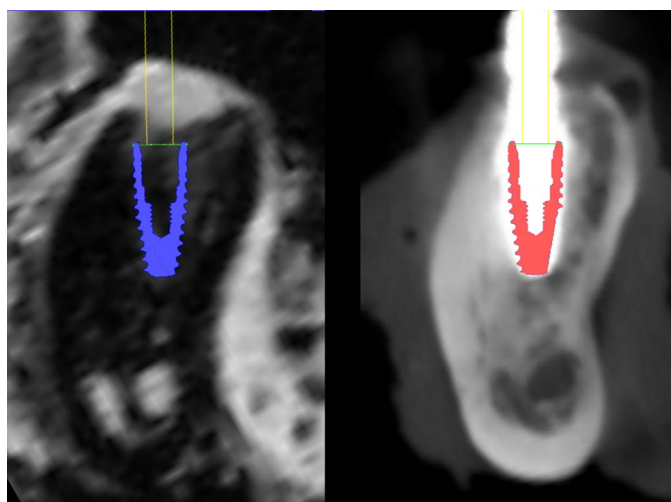
Optical imaging was performed with scan bodies (Cares Mono Scanbody, Art-Nr.025.4915, Straumann) that were connected to the implants and screw-retained with hand torque and scanned using the preoperative scanning protocol (Trios, 3Shape).

The evaluation of fully guided implant surgery was conducted with three different methods (Method 1, 2 and 3). Each evaluation method was performed by three examiners (GW, TF, FK).

In Method 1, the distances between the implant and relevant anatomical landmarks were measured using preoperative MRI and compared with the data retrieved from a postoperative CBCT. In Method 2, the preoperatively planned implant position was compared to the position of the implant assessed by CBCT. In Method 3, the preoperatively planned implant position was compared to the position of the implant assessed using an optical scan of the hemimandible with an implant scan body.

2.6.1 | Method 1

Distances between the planned implant and anatomical landmarks were measured in preoperative images and compared to distances between placed implants and respective landmarks in postoperative images (Figure 3). Manual measurements were performed by three examiners (GW, TF, FK). Each measurement was repeated three times. The following distances were assessed: implant apex – inferior alveolar nerve (nerve distance); implant shoulder – buccal bone (buccal bone); implant shoulder – lingual bone (lingual bone).

2.6.2 | Method 2

The postoperative CBCT scans were firstly aligned with preoperative MRI scans using common anatomical landmarks and radiopaque markers. Secondly, the implant displayed in postoperative CBCT images was manually aligned with the stored CAD-dataset of the implant. The deviation between the planned implant and the
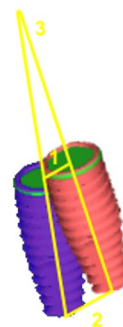
FIGURE 4 Assessment of deviation of planned implant (blue) in MR image (a) and actual implant (red) displayed with postoperative CBCT (b). The deviation between planned implant and actual implant is measured at the implant shoulder (1) and implant apex (2). The angular deviation (3) is calculated between the planned implant axis and the actual implant axis

postoperatively displayed implant was calculated by the software coDiagnostiX, Version 7 (Figure 4).

2.6.3 | Method 3

The postoperative optical scan containing a scan body was aligned with the preoperative optical scan on the basis of common surface characteristics and with the help of the radiopaque markers. The software calculated the deviation between planned and actual implant based on the alignment of optical scans (Figure 5).

For Method 2 and 3, the following parameters were assessed with the software tool: 3D deviation of implant shoulder (3D shoulder), 3D deviation of implant apex (3D apex), angular deviation of implant axes (angle).

2.7 | Statistical analysis

Descriptive analysis including standard deviation, minimum and maximum values were calculated. The overall results for deviation between planned and actual implant position were grouped for the method of measurement (Method 2 – CBCT, Method 3 – optical scan) and the dental status (single missing tooth, cantilever, edentulous). Mixed linear regression models were used for statistical analysis. Pair-wise comparison was performed with Scheffe-test. Intra and interexaminer variance were calculated. Statistical analysis was conducted with STATA Version 14.2 (StataCorp).

3 | RESULTS

MR imaging data in the DICOM-format were successfully imported into the implant planning software. The MR images displayed all relevant anatomical structures for dental implant planning such as cortical and cancellous portions of the alveolar bone, inferior alveolar nerve and adjacent teeth and gingiva. The software allowed the display of multiplanar reconstructions in axial, transversal and sagittal orientation. The dimensions of the alveolar bone were measured in axial, transversal and sagittal direction oriented along the prospective implant positions.

3.1 | Method 1

The results for the manual measurements are displayed in Table 1.

Manual measurements were significantly different between preoperative and postoperative images. The distance between implant apex and inferior alveolar nerve was on average 0.28 mm longer in postoperative assessment compared to preoperative measurements (CI 0.11–0.44 mm) ($p = .001$). The buccal bone thickness (implant shoulder – buccal bone outline) measured on postoperative images was on average 0.23 mm higher than in preoperative measurements (CI 0.07–0.38 mm) ($p = .04$). The lingual bone thickness (implant shoulder – lingual bone outline) measured on postoperative images was on average 0.25 mm higher than on preoperative images (CI 0.078–0.42 mm) ($p = .004$).

Manual measurements of distance between implant and inferior alveolar nerve and buccal bone thickness were not significantly influenced by the examiner. In preoperative and postoperative images, there was an interexaminer variance of $5.12e^{-1}$ and $1.34e^{-19}$, respectively. The intraexaminer variance was likewise not significant for pre- and postoperative measurements ($5.88e^{-20}$ and $7.83e^{-21}$). The preoperative measurement of lingual bone thickness was influenced by the examiner, resulting in an interexaminer variance of 0.042. The intraexaminer variance was not significant ($8.92e^{-16}$). Postoperative measurements of lingual bone thickness were not significantly different for interexaminer ($8.92e^{-16}$) and intraexaminer evaluation ($3.37e^{-22}$).
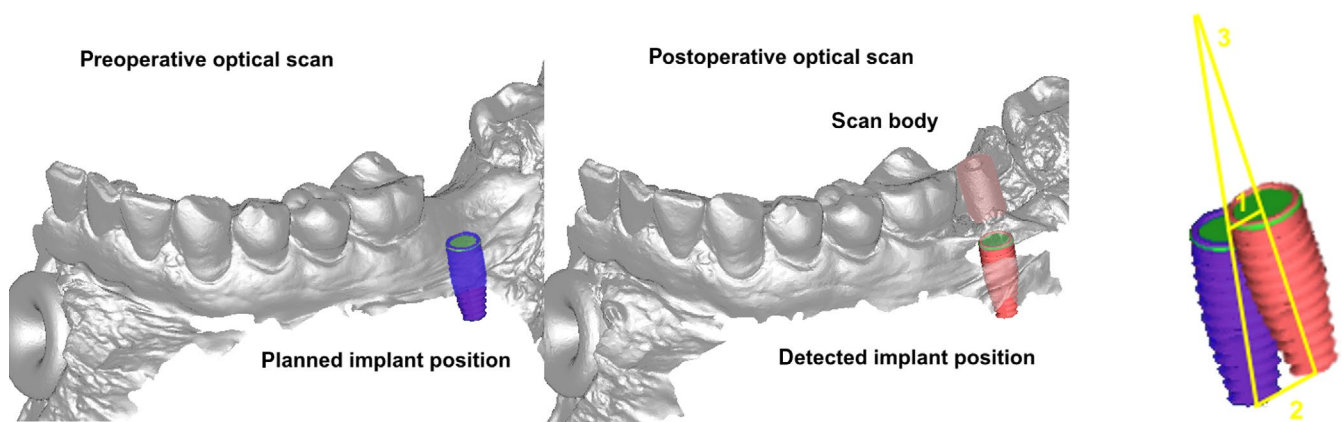
FIGURE 5 Preoperative optical scan with planned implant (blue), postoperative optical scan with scan body. The actual implant position (red) detected in the postoperative optical scan is compared to the planned implant position. The deviation between planned and actual implant position is assessed at implant shoulder (1) and implant apex (2) and between the implant axes (3), respectively

TABLE 1 Mean (standard deviation), minimum and maximum values in millimeters for manual measurements in preoperative and postoperative images

| Measurement | Anatomical situation | Preoperative planning (MRI) | | | Postoperative image (CBCT) | | | |
		Mean (*SD*)	Min	Max	Mean (*SD*)	Min	Max	*p*-value
Nerve distance	All	3.57 (2.24)	1.4	9.9	3.82 (2.49)	0	9.9	.001
	ST	6.47 (2.91)	2.5	9.9	6.07 (3.26)	1.8	9.9	
	PE	2.93 (0.96)	1.4	4.2	3.94 (1.02)	2.1	5.4	
	ED	2.35 (0.56)	1.4	3.3	1.99 (1.58)	0	5.1	
Buccal bone	All	0.94 (1.04)	0	4.3	1.16 (0.71)	0	3.1	.004
	ST	0.91 (0.94)	0	2.6	1.57 (1.04)	0	3.1	
	PE	0.93 (0.86)	0	2.8	1.04 (0.67)	0	2	
	ED	0.96 (1.23)	0	4.3	1.04 (0.4)	0	1.7	
Lingual bone	All	1.88 (1.33)	0	4.8	2.01 (1.26)	0.5	5.4	.004
	ST	2.60 (1.57)	0.8	4.8	3.10 (1.58)	1.5	5.4	
	PE	2.39 (1.10)	0.4	4.4	1.97 (1.17)	0.6	4.6	
	ED	0.87 (0.85)	0	3.5	1.58 (0.86)	0.5	3.6	

Note: Significance of deviation between pre- and postoperative measurements.

Abbreviations: ED, edentulous alveolar ridge; PE, partially edentulous cantilever situation; ST, single missing tooth.

3.2 | Method 2 and 3

Software-based assessment of implant positions using postoperative CBCT and postoperative optical scans resulted in measurements for the following parameters (Table 2).

The deviation between pre- and postoperative implant position was not significantly influenced by the dental status (single-tooth gaps, cantilever situations and edentulous situations). The examiner did not have an influence on the measurements.

The results for Method 2 and Method 3 were compared, and significant differences were found for the method for the 3D deviation of the implant shoulder. No significant differences were found for the 3D deviation of the implant apex and the angular deviation. The significance and mean deviation between the two assessment methods are displayed in Table 3.

4 | DISCUSSION

This study showed the successful use and accuracy of MRI for fully guided implant surgery in human mandibles in vitro. The study confirmed the first hypothesis, that dento-alveolar anatomy is sufficiently displayed using MR imaging with the given protocol, the second hypothesis that the workflow for fully guided implant surgery may be conducted using MRI data and optical surface scans and the third hypothesis that the accuracy of guided implant surgery based on MRI data is comparable to the respective workflow using CBCT data and optical surface scans.

The accuracy of virtual implant planning and fully guided implant placement using MRI was assessed with three different methods. Postoperative CBCT was used to compare results with previous studies. An assessment of implant positions was additionally performed with surface scans to verify the results with a second image modality. Manual measurements between implants and anatomical structures were performed to ensure that relevant anatomical structures were displayed with MRI and respected with the proposed workflow.

The accuracy of MRI-based fully guided implant placement was comparable to CBCT-based fully guided implant surgery as stated in two recent systematic reviews (Marlière, Demètrio, Picinini, Oliveira, & Netto, 2018; Tahmaseb, Wu, Wismeijer, Coucke, & Evans, 2018).

Tahmaseb et al. included studies using CBCT for postoperative evaluation. They documented a mean deviation between planned and actual implant position of 1.2 mm (CI 1.04–1.44) at the implant shoulder and 1.4 mm (CI 1.28–1.58) at the implant apex. This corresponds with the findings for CBCT evaluation (Method 2) with 3D deviations of 1.34 mm (*SD* 0.88 mm) at the implant shoulder and 1.41 mm (*SD* 0.84 mm) at the implant apex, respectively, in the present study. Tahmaseb et al. stated that higher deviations were found for fully guided implant placement in edentulous jaws: 1.3 mm (CI 1.09–1.56) at the implant shoulder and 1.5 mm (CI 1.29–1.62) at the implant apex. The present study included mostly edentulous jaws and mucosa-supported drill guides with mini implants that served as an additional support. The mean deviations in the subgroup of edentulous jaws were higher than in dentate groups with single-tooth gaps or cantilever situations: 1.51 mm (*SD* 1.04 mm) at the implant shoulder and 1.45 mm (*SD* 0.89 mm) at the implant apex (Tahmaseb et al., 2018).

Marlière et al. focused their systematic review on mucosa-supported drill guides with additional fixation screws in edentulous situations, comparable to anatomical situations in the present study. Mean deviations between planned and actual implant positions ranged between 0.71 mm (*SD* 0.4 mm) and 2.17 mm (*SD* 0.87 mm) at the implant shoulder, 0.77 mm (*SD* 0.38 mm) and 2.86 mm (*SD*

2.17 mm) at the implant apex, and 1.85 degrees (SD 0.75°) and 8.4 degrees (SD 4.2°) for angular deviation (Marlière et al., 2018).

Reported maximum deviations of implant positions for fully guided implant placement range between 1.3 and 4.0 mm (implant shoulder), 1.8 and 3.7 mm at the implant apex and 4.5° and 17.1° (angle), respectively (Schnutenhaus, Edelmann, Rudolph, & Luthhardt, 2016; Stübinger, Buitrago-Tellez, & Cantelmi, 2014;

TABLE 2 Mean values, Standard deviation (SD), minimal and maximum deviations for accuracy assessment based on CBCT and optical scans

Method	Anatomical situation	Mean	SD	Min	Max
3D shoulder (mm)					
2 (CBCT)	All	1.34	0.88	0.22	3.78
	ST	0.96	0.37	0.55	1.44
	PE	1.33	0.84	0.22	3.19
	ED	1.51	1.04	0.39	3.78
3 (optical scan)	All	1.03	0.46	0.49	2.39
	ST	0.65	0.18	0.49	0.98
	PE	1.11	0.62	0.54	2.39
	ED	1.12	0.27	0.72	1.73
3D apex (mm)					
2 (CBCT)	All	1.41	0.84	0.25	3.89
	ST	1.05	0.62	0.25	1.93
	PE	1.55	0.87	0.34	3.05
	ED	1.45	0.89	0.54	3.89
3 (optical scan)	All	1.28	0.52	0.45	2.46
	ST	1.04	0.22	0.77	1.28
	PE	1.32	0.58	0.59	2.46
	ED	1.34	0.56	0.45	2.43
Angle (degrees)					
2 (CBCT)	All	4.84	3.18	1.2	14.7
	ST	4.17	1.69	2.1	7.2
	PE	4.63	3.15	1.3	11.2
	ED	5.31	3.7	1.2	14.7
3 (optical scan)	All	4.21	2.01	0.8	8.6
	ST	4.15	1.67	2	6.1
	PE	3.33	1.38	0.8	5.3
	ED	4.99	2.33	0.8	8.6

Abbreviations: ED, edentulous alveolar ridge; PE, partially edentulous cantilever situation; ST, single missing tooth.

Vercruyssen et al., 2014; Verhamme et al., 2017). Lower deviations were found in situations with single-tooth gaps and higher deviations were found in edentulous jaws with either bone- or mucosa-supported drill guides involving anchor pins or bone fixation screws and flapless procedures. In this study, the maximum deviations of 3.8 mm (implant shoulder), 3.9 mm (implant apex) and 14.7° (angle) were as well documented for the edentulous hemimandibles and therefore correspond to the reported deviations.

In the literature, assessment of the implant position is mostly accomplished using a postoperative CBCT scan. This method was also used in this study. Additionally, postoperative optical scans were used for the assessment of accuracy. The comparison of both methods (postoperative CBCT and postoperative optical scan) showed significantly lower deviations for assessment with optical scans for one value (3D deviation at implant shoulder). This finding is in contrast to the finding of Skjerven, Olsen-Bergem, Rønold, Riis, and Ellingsen (2019) who found no significant differences between assessment with postoperative CBCT and postoperative optical scans using the same software and protocol as in this study (Skjerven et al., 2019). Skjerven et al. (2019) examined guided implant surgery in partially edentulous patients with tooth-supported drill guides and found mean 3D deviations of 0.9 mm (SD 0.44 mm) at the implant shoulder and 1.11 mm (SD 0.44 mm) for CBCT evaluation. Evaluation with intraoral scans showed mean 3D deviations at the implant shoulder of 0.87 mm (SD 0.39 mm) and 1.07 mm (SD 0.39 mm) at the implant apex. These data were comparable to deviations found for single-tooth spaces in the present study. The difference between the study of Skjerven et al. (2019) and this study was that here preoperative MRI data was aligned with postoperative CBCT data and Skjerven et al. (2019) aligned preoperative and postoperative CBCT data. The accuracy of aligning two CBCT datasets may be higher than aligning MRI and CBCT data.

To assess the accuracy of fully guided implant placement despite of alignment errors of pre- and postoperative imaging data, an alternative assessment method was applied. Manual measurements of relevant distances between implants and anatomical structures were performed in preoperative MR images and in postoperative CBCT images. Minimum distances between implants and relevant anatomical structures were regarded in preoperative implant planning and were confirmed in postoperative assessment. The distances between implant apex and inferior alveolar nerve, the buccal and lingual bone lamella, respectively, showed higher values in postoperative assessment. The overestimation of distances between structures in CBCT is in conformity with previously published studies

TABLE 3 Comparison between accuracy assessment with CBCT and optical scans

	Comparison Method 2 (CBCT) and Method 3 (optical scan), p-value	Mean deviation in mm (Confidence interval)
3D shoulder	.001	0.31 (0.12–0.49)
3D apex	.14	
Angle	.22	

Note: p-values for significance and mean deviation between the assessment methods for each parameter.

documenting a measurement bias between 0.39 and 0.53 mm in CBCT images (Dings et al., 2019). A systematic review on the accuracy of linear measurements in CBCT and multi slice CT images summarized measurement deviations to a value below one millimeter and found over and underestimation of measurements. (Fokas, Vaughn, Scarfe, & Bornstein, 2018). Therefore, the overestimation of distances in postoperative CBCT images in this study is within the reported measurement tolerance.

The workflow of fully guided implant placement using drill guides requires the acquisition of CBCT and optical scans of the teeth and mucosal surfaces. The alignment of both datasets is prone to errors due to imaging artifacts in CBCT originating from the tooth surface (Flügge et al., 2017). For fully guided implant placement on the basis of MR imaging data, optical scans are as well required. Especially, in edentulous patients the alignment process could be facilitated due to the fact, that both MRI data and optical scans display the soft tissue surface that might be used as a common anatomical structure for alignment. MRI might therefore pose a valuable alternative for fully guided implant placement in edentulous patients as it overcomes the major limitation of missing information on soft tissues in CBCT. In this study alignment was performed with the help of mucosal surfaces and radiopaque markers, delivering landmarks as corresponding characteristics displayed both in MRI and optical scan data.

MR imaging has the major advantage that it does not apply ionizing radiation. Furthermore, MRI is advantageous due to its display of soft tissues, however, its routine application in dentistry has been limited to the visualization of the temporomandibular joint (Cuccia, Caradonna, Bruschetta, Vaccarino, & Milardi, 2014; Liedberg, Panmekiate, Petersson, & Rohlin, 1996). The lack of the display of hard tissues, for example, teeth, cortical bone is one limiting factor for a broader use of MRI in dentistry along with its high cost and limited availability. MRI systems are operated in specialized clinics and require extensive hardware and specially trained radiologists. Technological developments are therefore needed to make use of MRI in dentistry.

MRI with traditional imaging protocols has been used for imaging and measurement of the alveolar bone prior to implant placement. Long acquisition times of up to 30 min and low image quality due to an inadequate resolution (slice thickness 2–4 mm) have not proven useful for clinical routine and adoption using virtual implant planning software (Gray, Redpath, & Smith, 1996; Gray, Redpath, Smith, & Staff, 2003). One recent case study reported on the use of MRI for virtual implant planning and fully guided implant placement in patients and introduced an imaging protocol for clinical routine (Flügge et al., 2020). Novel imaging protocols and their adaptation to the specifics of the dento-alveolar complex have led to a gaining clinical relevance of MRI (Hövener et al., 2012; Ludwig et al., 2016). The adoption of dedicated imaging protocols and hardware advanced resolution in MR images, however, (CB)CT often has a higher resolution than MRI. MRI is useful to display dental roots with the internal dental pulp and the surrounding periodontal ligament, cancellous bone and cortical bone through the surrounding soft tissues as well as the intraosseous course of the inferior alveolar nerve and the

intraoral gingiva and mucosa (Flügge et al., 2016; Gradl et al., 2017; Kreutner et al., 2017; Wanner, Ludwig, Hövener, Nelson, & Flügge, 2018).

Limitations of MR imaging include artifacts in the presence of ferromagnetic materials (Tymofiyeva et al., 2013). This is especially relevant in patients with existing dental restorations and might hinder adequate diagnostics. Methods for reduction of metal artefacts have already been proposed and applied for dental application, but strongly depend on the restoration material (Hilgenfeld et al., 2018). Although titanium implants do not cause major artifacts in MRI, this study used postoperative CBCT imaging for accuracy assessment. This was mainly due to the fact that comparability of accuracy results was only given with CBCT as previous studies used CBCT for postoperative assessment of implant positions.

The present study is the first study to confirm the accuracy of fully guided implant placement based on MR imaging data. However, this novel method was adopted in human mandibles ex vivo. The use of MRI for implant planning in vivo might result in higher deviations compared to the experimental set-up of this study. Further studies, focusing on the clinical use of MRI and fully guided implant surgery in humans have to be conducted to support the findings of this study.

5 | CONCLUSION

Relevant anatomical structures of the dento-alveolar complex for preoperative imaging diagnostics in implant dentistry are displayed with MRI. MRI data and optical scans might be aligned on the basis of the common anatomical landmarks. The workflow of virtual implant planning and drill guide design and fabrication might be performed with MRI. The accuracy of MRI-based fully guided implant placement in vitro is comparable to the conventional workflow using CBCT. So far specialized clinics with extensive hardware are required for MR examinations. Therefore, MRI is not available for daily routine imaging in dentistry.

ORCID
Tabea Flügge https://orcid.org/0000-0002-1288-8452
Ute Ludwig https://orcid.org/0000-0002-0526-5935
Florian Kernen https://orcid.org/0000-0002-3067-0756

REFERENCES
Bracher, A. K., Hofmann, C., Bornstedt, A., Boujraf, S., Hell, E., Ulrici, J., … Rasche, V. (2011). Feasibility of ultra-short echo time (UTE) magnetic resonance imaging for identification of carious lesions. *Magnetic Resonance in Medicine*, 66(2), 538–545. https://doi.org/10.1002/mrm.22828

Cuccia, A. M., Caradonna, C., Bruschetta, D., Vaccarino, G., & Milardi, D. (2014). Imaging of temporomandibular joint: Approach by direct

volume rendering. *Journal of Clinical and Diagnostic Research*, 8(11), 105–109. https://doi.org/10.7860/JCDR/2014/9977.5195

Dings, J. P., Verhamme, L., Merkx, M. A., Xi, T., Meijer, G. J., & Maal, T. J. (2019). Reliability and accuracy of cone beam computed tomography versus conventional multidetector computed tomography for image-guided craniofacial implant planning: An in vitro study. *The International Journal of Oral and Maxillofacial Implants*, 34(3), 665–672. https://doi.org/10.11607/jomi.6915

Flügge, T., Derksen, W., Te Poel, J., Hassan, B., Nelson, K., & Wismeijer, D. (2017). Registration of cone beam computed tomography data and intraoral surface scans - A prerequisite for guided implant surgery with CAD/CAM drilling guides. *Clinical Oral Implants Research*, 28(9), 1113–1118. https://doi.org/10.1111/clr.12925

Flügge, T., Hövener, J.-B, Ludwig, U., Eisenbeiss, A.-K., Spittau, B., Hennig, J., ... Nelson, K. (2016). Magnetic resonance imaging of intraoral hard and soft tissues using an intraoral coil and FLASH sequences. *European Radiology*, 26(12), 4616–4623. https://doi.org/10.1007/s00330-016-4254-1

Flügge, T., Ludwig, U., Hövener, J. B., Kohal, R., Wismeijer, D., & Nelson, K. (2020). Virtual implant planning and fully guided implant surgery using magnetic resonance imaging—Proof of principle. *Clinical Oral Implants Research*, 31(6), 575–583. https://doi.org/10.1111/clr.13592

Flügge, T. V., Nelson, K., Schmelzeisen, R., & Metzger, M. C. (2013). Three-dimensional plotting and printing of an implant drilling guide: Simplifying guided implant surgery. *Journal of Oral and Maxillofacial Surgery*, 71(8), 1340–1346. https://doi.org/10.1016/j.joms.2013.04.010

Fokas, G., Vaughn, V. M., Scarfe, W. C., & Bornstein, M. M. (2018). Accuracy of linear measurements on CBCT images related to presurgical implant treatment planning: A systematic review. *Clinical Oral Implants Research*, 29(Suppl 16), 393–415. https://doi.org/10.1111/clr.13142

Gradl, J., Höreth, M., Pfefferle, T., Prager, M., Hilgenfeld, T., Gareis, D., ... Hähnel, S. (2017). Application of a dedicated surface coil in dental mri provides superior image quality in comparison with a standard coil. *Clinical Neuroradiology*, 27(3), 371–378. https://doi.org/10.1007/s00062-016-0500-9

Gray, C. F., Redpath, T. W., & Smith, F. W. (1996). Pre-surgical dental implant assessment by magnetic resonance imaging. *Journal of Oral Implantology*, 22(2), 147–153.

Gray, C. F., Redpath, T. W., Smith, F. W., & Staff, R. T. (2003). Advanced imaging: Magnetic resonance imaging in implant dentistry. *Clinical Oral Implants Research*, 14, 18–27.

Gruwel, M. L. H., Latta, P., Tanasiewicz, M., Volotovskyy, V., Šramek, M., & Tomanek, B. (2007). MR imaging of teeth using a silent single point imaging technique. *Applied Physics A*, 88(4), 763–767. https://doi.org/10.1007/s00339-007-4066-x

Hilgenfeld, T., Prager, M., Schwindling, F. S., Nittka, M., Rammelsberg, P., Bendszus, M., ... Juerchott, A. (2018). MSVAT-SPACE-STIR and SEMAC-STIR for reduction of metallic artifacts in 3T Head and neck MRI. *American Journal of Neuroradiology*, 39(7), 1322–1329. https://doi.org/10.3174/ajnr.A5678

Hövener, J.-B., Zwick, S., Leupold, J., Eisenbeiβ, A.-K., Scheifele, C., Schellenberger, F., ... Ludwig, U. (2012). Dental MRI: Imaging of soft and solid components without ionizing radiation. *Journal of Magnetic Resonance Imaging*, 36(4), 841–846. https://doi.org/10.1002/jmri.23712

Idiyatullin, D., Corum, C., Moeller, S., Prasad, H. S., Garwood, M., & Nixdorf, D. R. (2011). Dental magnetic resonance imaging: Making the invisible visible. *Journal of Endodontics*, 37(6), 745–752. https://doi.org/10.1016/j.joen.2011.02.022

Idiyatullin, D., Corum, C. A., Nixdorf, D. R., & Garwood, M. (2014). Intraoral approach for imaging teeth using the transverse B field

components of an occlusally oriented loop coil. *Magnetic Resonance in Medicine*, 72(1), 160–522. https://doi.org/10.1002/mrm.24893

Kreutner, J., Hopfgartner, A., Weber, D., Boldt, J., Rottner, K., Richter, E., & Haddad, D. (2017). High isotropic resolution magnetic resonance imaging of the mandibular canal at 1.5 T: A comparison of gradient and spin echo sequences. *Dentomaxillofacial Radiology*, 46(2), 20160268. https://doi.org/10.1259/dmfr.20160268

Liedberg, J., Panmekiate, S., Petersson, A., & Rohlin, M. (1996). Evidence-based evaluation of three imaging methods for the temporomandibular disc. *Dentomaxillofacial Radiology*, 25(5), 234–241. https://doi.org/10.1259/dmfr.25.5.9161176

Ludwig, U., Eisenbeiss, A. K., Scheifele, C., Nelson, K., Bock, M., Hennig, J., ... Hövener, J. B. (2016). Dental MRI using wireless intraoral coils. *Scientific Reports*, 6, 23301. https://doi.org/10.1038/srep23301

Marlière, D. A. A., Demètrio, M. S., Picinini, L. S., Oliveira, R. G., & Netto, H. D. M. C. (2018). Accuracy of computer-aided surgery for dental implant placement in fully edentulous patients: A systematic review. *European Journal of Dentistry*, 12(1), 153–160. https://doi.org/10.4103/ejd_249_17

Nkenke, E., Zachow, S., Benz, M., Maier, T., Veit, K., Kramer, M., ... Lell, M. (2004). Fusion of computed tomography data and optical 3D images of the dentition for streak artefact correction in the simulation of orthognathic surgery. *Dentomaxillofacial Radiology*, 33(4), 226–232. https://doi.org/10.1259/dmfr/27071199

Schnutenhaus, S., Edelmann, C., Rudolph, H., & Luthardt, R. G. (2016). Retrospective study to determine the accuracy of template-guided implant placement using a novel nonradiologic evaluation method. *Oral Surgery, Oral Medicine, Oral Pathology, and Oral Radiology*, 121(4), e72–e79. https://doi.org/10.1016/j.oooo.2015.12.012

Schulze, R., Heil, U., Gross, D., Bruellmann, D. D., Dranischnikow, E., Schwanecke, U., & Schoemer, E. (2011). Artefacts in CBCT: A review. *Dentomaxillofacial Radiology*, 40(5), 265–273. https://doi.org/10.1259/dmfr/30642039

Skjerven, H., Olsen-Bergem, H., Rønold, H. J., Riis, U. H., & Ellingsen, J. E. (2019). Comparison of postoperative intraoral scan versus cone beam computerised tomography to measure accuracy of guided implant placement-A prospective clinical study. *Clinical Oral Implants Research*, 30(6), 531–541. https://doi.org/10.1111/clr.13438

Stübinger, S., Buitrago-Tellez, C., & Cantelmi, G. (2014). Deviations between placed and planned implant positions: An accuracy pilot study of skeletally supported stereolithographic surgical templates. *Clinical Implant Dentistry and Related Research*, 16(4), 540–551. https://doi.org/10.1111/cid.12019

Tahmaseb, A., Wu, V., Wismeijer, D., Coucke, W., & Evans, C. (2018). The accuracy of static computer-aided implant surgery: A systematic review and meta-analysis. *Clinical Oral Implants Research*, 29(Suppl 16), 416–435. https://doi.org/10.1111/clr.13346

Tymofiyeva, O., Boldt, J., Rottner, K., Schmid, F., Richter, E. J., & Jakob, P. M. (2009). High-resolution 3D magnetic resonance imaging and quantification of carious lesions and dental pulp in vivo. *Magnetic Resonance Materials in Physics, Biology and Medicine*, 22(6), 365–374. https://doi.org/10.1007/s10334-009-0188-9

Tymofiyeva, O., Rottner, K., Gareis, D., Boldt, J., Schmid, F., Lopez, M. A., ... Jakob, P. M. (2008). In vivo MRI-based dental impression using an intraoral RF receiver coil. *Concepts in Magnetic Resonance Part B: Magnetic Resonance Engineering: An Educational Journal*, 33(4), 244–251. https://doi.org/10.1002/cmr.b.20126

Tymofiyeva, O., Vaegler, S., Rottner, K., Boldt, J., Hopfgartner, A. J., Proff, P. C., ... Jakob, P. M. (2013). Influence of dental materials on dental MRI. *Dentomaxillofacial Radiology*, 42(6), 20120271. https://doi.org/10.1259/dmfr.20120271

Vercruyssen, M., Cox, C., Coucke, W., Naert, I., Jacobs, R., & Quirynen, M. (2014). A randomized clinical trial comparing guided implant surgery (bone- or mucosa-supported) with mental navigation or the use

of a pilot-drill template. *Journal of Clinical Periodontoly, 41*(7), 717–723. https://doi.org/10.1111/jcpe.12231

Verhamme, L. M., Meijer, G. J., Bergé, S. J., Soehardi, R. A., Xi, T., de Haan, A. F. J., ... Maal, T. J. J. (2017). An accuracy study of computer-planned implant placement in the augmented maxilla using mucosa-supported surgical templates. *Clinical Implant Dentistry and Related Research, 17*(6), 1154–1163. https://doi.org/10.1111/cid.12230

Wanner, L., Ludwig, U., Hövener, J. B., Nelson, K., & Flügge, T. (2018). Magnetic resonance imaging – a diagnostic tool in postoperative evaluation of dental implants: A case report. *Oral Surgery, Oral Medicine, Oral Pathology, and Oral Radiology, 125*(4), e103–e107. https://doi.org/10.1111/cid.12230

Weiger, M., Pruessmann, K. P., Bracher, A.-K., Köhler, S., Lehmann, V., Wolfram, U., ... Rasche, V. (2012). High-resolution ZTE imaging of human teeth. *NMR in Biomedicine, 25*(10), 1144–1151. https://doi.org/10.1002/nbm.2783

SUPPORTING INFORMATION

Additional supporting information may be found online in the Supporting Information section.

How to cite this article: Flügge T, Ludwig U, Winter G, Amrein P, Kernen F, Nelson K. Fully guided implant surgery using Magnetic Resonance Imaging – An in vitro study on accuracy in human mandibles. *Clin Oral Impl Res.* 2020;31: 737–746. https://doi.org/10.1111/clr.13622